J. Fluid Mech. (1991), *vol.* 230, *pp.* 75–95
Printed in Great Britain

Intermittent dynamics in simple models of the turbulent wall layer

By GAL BERKOOZ[1], PHILIP HOLMES[2] AND J. L. LUMLEY[3]

[1] Center for Applied Mathematics, Ithaca, NY 14853-7501, USA

[2] Departments of Theoretical and Applied Mechanics and Mathematics, Ithaca, NY 14853-7501, USA

[3] Sibley School of Mechanical and Aerospace Engineering, Ithaca, NY 14853-7501, USA

(Received 22 January 1990 and in revised form 19 February 1991)

We generalize the class of models of the wall layer of Aubry *et al.* (1988), based on the proper orthogonal decomposition, to permit uncoupled evolution of streamwise and cross-stream disturbances. Since the Reynolds stress is no longer constrained, in the absence of streamwise spatial variations all perturbation velocity components eventually decay to zero. However, their transient behaviour is dominated by 'ghosts' of the non-trivial fixed points and attracting heteroclinic cycles which are characteristic features of those models based on empirical eigenfunctions whose individual velocity components are fixed. This suggests that the intermittent events observed in Aubry *et al.* do not arise solely because of the effective closure assumption incorporated in those models, but are rooted deeper in the dynamical phenomenon of the wall region.

1. Introduction

In the recent paper of Aubry *et al.* (1988) a low-dimensional model for the dynamical interaction of streamwise vortices in the wall region of a turbulent boundary layer was derived. The model made use of the proper orthogonal, or Karhunen–Loève, decomposition theorem (Lumley 1967, 1970), which provides a basis of divergence free empirical eigenfunctions for the space of velocity fields. The Navier–Stokes equations were then projected, via the Galerkin method (cf. Ladyzhenskaya 1969; Téman 1988) into a sequence of subspaces spanned by finite (and small) sets of these eigenfunctions. The resulting sets of ordinary differential equations in the modal amplitude coefficients, obtained by truncating at various orders, were then studied by the methods of dynamical systems theory.

The basis functions derived from experimental autocorrelation measurements via proper orthogonal decomposition (cf. Herzog 1986) are optimal in the sense that, among all possible reconstructions of velocity fields by any basis set truncated at some fixed order, they yield the greatest kinetic energy in a time-averaged sense for 'typical' flows under the same conditions as those for which the eigenfunctions were derived. There is increasing evidence, based primarily upon direct numerical simulations of the Navier–Stokes equations, that these empirical eigenfunctions offer significant advantages over *a priori* choices of bases such as Fourier or Chebyshev modes or eigenfunctions of the Stokes operator itself. See Moin & Moser (1989), Sirovich (1989), Kirby, Boris & Sirovich (1990) and references therein. We therefore expect the finite dimensional dynamical systems thus obtained to capture important

aspects of the turbulent energy production mechanism, even at relatively low truncation orders, provided that suitable account is taken of energy loss to neglected modes in the inertial and dissipative ranges. For more details of and comments on the procedure, see the references cited above or Holmes (1990).

The particular truncation which was studied in detail by Aubry *et al.* (1988) includes no streamwise variations. (Since the typical lengthscales of cross-stream and streamwise disturbances differ by an order of magnitude in the wall region, it was felt that this was a reasonable first approximation.) However, streamwise variations enter the model indirectly in that the empirical eigenfunctions, which are *vector valued*, are derived from time-averaged autocorrelation measurements made in a turbulent boundary layer in which (long wavelength) streamwise disturbances play a prominent role. This results in eigenfunction components whose magnitudes at streamwise wavenumber zero reflect the average Reynolds stress $\langle u_1 u_2 \rangle$ in the wall region. While in principle the empirical eigenfunctions yield a complete basis, when low-order truncations are employed the effect is to constrain admissible velocity fields by coupling cross-stream and streamwise components. This is equivalent to a closure assumption, as shown below.

Specifically, the representation of the velocity field employed by Aubry *et al.* (1988), restricted to zero streamwise wavenumber ($k_1 = 0$) and a single family of eigenfunctions, was

$$\boldsymbol{u}(\boldsymbol{x}, t) = \sum_{k=-K}^{K} a_k(t) \exp(2\pi i k x_3 / L_3)\, \boldsymbol{\phi}_k(x_2). \tag{1.1}$$

Here $x_1(u_1)$ is the streamwise direction, $x_3(u_3)$ the spanwise and $x_2(u_2)$ the direction normal to the wall and k/L_3 is the spanwise wavenumber. Each basis element $\boldsymbol{\phi}_k = (\phi_{1_k}, \phi_{2_k}, \phi_{3_k})$ is a divergence-free, time-independent vector field. Typical forms of the components $\phi_{j_k}(x_2)$ are shown in Aubry *et al.* (1988, figure 4): note that (for $k_1 = 0$) they are purely real or purely imaginary. The complex modal coefficients $a_k(t)$ are determined via solution of the projected ordinary differential equations and the sum in (1.1) is taken over a discrete set of spanwise Fourier modes.

Since the velocity field $\boldsymbol{u}$ is real, it is only necessary to consider coefficients a_k with $k \geqslant 0$. Moreover, as described in Aubry *et al.* (1988), the coefficient a_0, which represents a modification to the (constant) mean velocity profile, evolves autonomously and decays to zero as t increases and it can therefore be dropped in studies of long-term behaviour. One therefore studies the behaviour of the K 'active' modes $a_1, \ldots, a_k$. The general form of the projected differential equations determining the modal amplitude vector $\boldsymbol{a} = (a_1, \ldots, a_k)^{\mathrm{T}}$ is

$$\dot{\boldsymbol{a}} = \boldsymbol{A}_\alpha \boldsymbol{a} + \boldsymbol{B}_\alpha(\boldsymbol{a}, \boldsymbol{a}) + \boldsymbol{C}(\boldsymbol{a}, \boldsymbol{a}, \boldsymbol{a}). \tag{1.2}$$

Here $\boldsymbol{A}_\alpha$ is a diagonal matrix with entries involving negative (stabilizing) contributions from viscous dissipation in the modes included in (1.1) and losses, parameterized by α, to neglected modes as well as positive contributions from energy production terms, to be discussed below. $\boldsymbol{B}_\alpha$ is a quadratic interaction term derived from the nonlinear term of the Navier–Stokes equation and $\boldsymbol{C}$ is a cubic term which results from expressing the mean velocity profile as a function of the amplitude of the perturbation velocity field. Specifically, we take

$$U_1(x_2) = \frac{u_\tau^2}{\nu}\left(x_2 - \frac{x_2^2}{H}\right) + \frac{1}{\nu}\int_0^{x_2} \langle u_1 u_2 \rangle \, \mathrm{d}x_2. \tag{1.3}$$

This is the solution of the exact equation for the mean velocity profile (using spatial

averages in planes parallel to the wall), making only the assumption that the changes in the mean velocity are slow in some sense. The first term in (1.3) represents the driving pressure gradient. The second term describes the erosion of the mean velocity gradient by the momentum transport due to the perturbation velocity field. This has a globally stabilizing effect; as the eddies grow more energetic, they reduce the mean velocity gradient, cutting off their source of energy.

For (unrealistically) large loss α, the trivial solution $\boldsymbol{a} = \boldsymbol{0}(\boldsymbol{u} = \boldsymbol{0})$ of (1.2) is globally asymptotically stable. As α decreases, the entries of $\boldsymbol{A}_\alpha$ (which are of the form $a_{kk} - \alpha(a'_{kk} + a''_{kk})$; $a_{kk}, a'_{kk}, a''_{kk} > 0$) successively become positive and non-trivial branches of equilibria bifurcate from $\boldsymbol{0}$. (The dependence of $\boldsymbol{B}_\alpha$ on α is relatively weak.) These branches subsequently undergo secondary bifurcations and become unstable. The full picture is rather complicated and depends delicately on the precise coefficients of $\boldsymbol{A}_\alpha$, $\boldsymbol{B}_\alpha$, $\boldsymbol{C}$, which themselves depend on the wavenumbers of modes selected via the cross-stream period L_3 (cf. (1.1)): see Aubry & Sanghi (1989), Aubry, Holmes & Lumley (1990), and Stone (1989). However, a robust feature of all the models studied so far is the existence of open ranges of loss parameter α in which the systems possess *attracting heteroclinic cycles*.

A *heteroclinic orbit* is a solution connecting two equilibrium points of an ordinary or partial differential equation. A heteroclinic cycle is a set of two or more such connections which closes up, so that nearby solutions circulate and continually return to neighbourhoods of the equilibria. These latter are necessary unstable saddle points. It is easy to show that such cycles cannot generally exist in 'typical' (generic) differential equations, since they are unstable to small perturbations such as parameter variation (cf. Guckenheimer & Holmes 1983). However, as Guckenheimer & Holmes (1988) realized, symmetries in the equations can 'stabilize' heteroclinic cycles and subsequently the existence of structurally stable cycles, occurring for open sets of parameter values, was proved for systems with both discrete and continuous symmetry groups (see also Armbruster, Guckenheimer & Holmes 1988, 1989).

When a heteroclinic cycle is attractive, solutions in its neighbourhood spend long quiescent periods near the equilibria, punctuated by rapid heteroclinic transits. This phase space behaviour corresponds in physical space to periods of (pseudo-) steady flow involving fewer modes interspersed with relatively violent 'events' in which (many) more modes become active. Numerical solutions of the one-space dimension Kuramoto–Sivashinsky equation due to Hyman & Nicolaenko (1985) and Hyman, Nicolaenko & Zaleski (1986) (cf. Nicolaenko, Scheurer & Téman 1985, 1986) had already been observed to exhibit such behaviour, which has more recently been seen in simulation of the two-space dimension Kolmogorov flow (Nicolaenko & She 1990*a*, *b*). At about the same time that Armbruster *et al.* (1988) did their work, Proctor & Jones (1988; cf. Jones & Proctor 1987) found symmetric heteroclinic cycles in a two-mode reduction of a Bénard convection problem. In fact Busse & Heikes (1980) and Busse (1981) had even earlier seen cycles due to the discrete group of cyclic permutations in a model for three interacting modes.

In the present case the continuous symmetry group $O(2)$ in phase space – the group of reflections and rotations in a plane – arises naturally from the invariance under spanwise translations and reflections of the original boundary-layer flow. Similar symmetries arise in weakly nonlinear evolution equations, such as those of Ginzburg, Landau, Newell, Segal and Whitehead, which describe modal interactions in transition flows. See Holmes (1991) for a partial review.

As described in Aubry *et al.* (1988) and Holmes (1990), the velocity fields $\boldsymbol{u}(\boldsymbol{x}, t)$ reconstructed in (1.1) with coefficients $a_k(t)$ undergoing such cycles have much in

common with the bursting phenomenon observed in turbulent boundary layers (cf. Kline *et al.* 1967; Corino & Brodkey 1969). In particular, the roll spacing is that observed by Kline *et al.*, and it is possible to adjust the loss to unresolved disturbances so that the bursting period is also that observed by Kline *et al.* When this is done, the duration of the burst also agrees with Kline's observations. An event consists of a sudden intensification and sharpening of the updraft between eddies, followed by a drawing apart of the eddies, and the establishment of a gentle downdraft between them. These are similar respectively to the ejection and sweep events that are observed. The rolls shift sidewise by an amount approximately equal to the roll spacing during a burst, a phenomenon also noted by Kline. There are many other points of contact between our model and observation, which have been detailed elsewhere (Aubry & Sanghi 1989, 1990; Aubry *et al.* 1990). It is therefore important to establish that the cycles are not merely artefacts of a low-dimensional truncation. In particular, as Moffatt (1990) pointed out, if streamwise and cross-stream velocity components are allowed to evolve independently, then all disturbances eventually decay in the absence of streamwise variations. This appears to be well known and may be demonstrated directly from the Navier–Stokes equations by showing that, in the absence of streamwise variations, the evolution of the cross-stream (u_2, u_3) velocity components is decoupled from that of the streamwise (u_1) component and that the former experiences no energy input from the mean shear $(\partial U_1/\partial x_2)$. Details may be found in Moffatt (1990). Alternatively, one may seek a exact solution of the Navier–Stokes equations containing time-dependent streamwise vortices of the form

$$u_2 = \psi_{,3} = A(t)\cos kx_3 \sin kx_2, \quad u_3 = -\psi_{,2} = -A(t)\sin kx_3 \cos kx_2, \quad u_1 = -u_2, \tag{1.4}$$

with a fixed uniform shear and show directly that the amplitude of the cross-stream components decays monotonically and the streamwise component, after an initial increase in amplitude, also eventually decays. This features reappears in an unconstrained version of our model discussed below. Also see the comments following (3.13). Physically, unless the ratio of Reynolds stress to energy is held above zero, as it is by the representation (1.1), then the disturbance cannot continue to extract energy from the mean flow. In the present paper we address this aspect of our earlier model and present a model in which uncoupled evolution of velocity components is permitted. We show that, while the disturbances do decay correctly in such a model, their transient dynamics is dominated by echoes of the non-trivial fixed points and the associated heteroclinic cycles.

The paper is organized as follows. In §2 we review the symmetries inherited by the projected equations (1.2) from the original flow and show how heteroclinic cycles arise in the Aubry *et al.* 'coupled' models. In §3 we specifically identify the energy production terms in the original models and show how they reappear in a class of models with uncoupled velocity components. We also include a discussion of the physical origin of the non-trivial fixed points and cycles in the original models in terms of the Reynolds stress/energy ratio. We argue that in those models a closure assumption was effectively made in which the effects of streamwise variations were incorporated into the representation (1.1). Section 4 deals with an 'uncoupled' model. It is shown analytically that decaying heteroclinic cycles exist and numerical simulations are also presented. We draw conclusions in §5.

For more information on heteroclinic orbits and dynamical systems in general, see Guckenheimer & Holmes (1983). For a review of heteroclinic cycles and their

relevance to intermittency in turbulence production, see Holmes (1991), where references to work such as that of Newell, Rand & Russell (1988) on Langmuir turbulence in plasmas can be found.

2. $O(2)$ symmetry and heteroclinic cycles

To review the heteroclinic cycles found by Aubry *et al.* (1988), we discuss the special case of a model involving only two spanwise modes ($K = 2$ in (1.1)). As that paper and Aubry & Sanghi (1989, 1990) show, this minimal model contains the essence of higher-dimensional truncations.

In this case the equations of motion (1.2) take the form:

$$\left.\begin{aligned} \dot{a}_1 &= \mu_1 a_1 + \beta_{12} a_1^* a_2 + (e_{11}|a_1|^2 + e_{12}|a_2|^2) a_1, \\ \dot{a}_2 &= \mu_2 a_2 + \beta_{21} a_1^2 + (e_{21}|a_1|^2 + e_{22}|a_2|^2) a_2. \end{aligned}\right\} \tag{2.1}$$

Here $a_j = x_j + \mathrm{i}y_j$ are the complex coefficients, * denotes complex conjugate and the parameters μ_j, β_{ij}, e_{ij} are all real numbers resulting from integrals of products of eigenfunction components and their derivatives (cf. Aubry *et al.* 1988, Appendix A). This model, involving the interaction of two complex Fourier modes having wavenumbers in ratio 1:2, is amenable to fairly complete mathematical analysis. In particular, Armbruster *et al.* (1988, cf. 1989) make use of the fact that the system

$$\left.\begin{aligned} \dot{a}_1 &= \beta_{12} a_1^* a_2, \\ \dot{a}_2 &= \beta_{21} a_1^2, \end{aligned}\right\} \tag{2.2}$$

is completely integrable, with constants of motion

$$E = -\beta_{21}|a_1|^2 + \beta_{12}|a_2|^2, \quad L = \mathrm{Im}\,(a_1 a_2^* - a_1^* a_2), \tag{2.3a, b}$$

to study (2.1) for μ_j, a_j small by perturbation and averaging techniques.

The symmetry properties of (2.1–2.2) are of crucial importance. Note that these equations are invariant under rotation

$$a_j \to a_j \mathrm{e}^{\mathrm{i}j\nu} \tag{2.4a}$$

and the complex conjugation

$$a_j \to a_j^*. \tag{2.4b}$$

These symmetries in Fourier space ($O(2)$ – equivariance) are simply the result of translation ($x_3 \to x_3 + d$) and reflection ($x_3 \to -x_3$), $(u_1, u_2, u_3) \to (u_1, u_2, -u_3)$ invariance of the Navier–Stokes equation for the perturbation velocity $\boldsymbol{u}$ in physical space.

The heteroclinic cycles occur as follows. For $e_{ij} < 0$, $\beta_{21} < 0 < \beta_{12}$ and $\mu_2 > 0$, $\mu_1 \approx 0$, (2.1) has a circle $\{|a_2| = (-\mu_2(e_{22})^{\frac{1}{2}}, a_1 = 0\}$ of non-trivial equilbria which are (unstable) saddle points. That circles of such equilibria occur is a direct consequence of (2.4*a*). Now consider the restriction of (2.1) to the invariant real subspace $(a_1, a_2) = (x_1 + \mathrm{i}.0, x_2 + \mathrm{i}.0)$. In this plane, the two equilibria

$$(x_1, x_2) = (0, \pm(-\mu_2/e_{22})^{\frac{1}{2}}, \tag{2.5}$$

are, respectively, a saddle and a sink and it is not hard to show that the unstable manifolds (separatrices) of the saddle $A: x_2 = +(-\mu_2/e_{22})^{\frac{1}{2}}$ connect it to the sink $B: x_2 = -(-\mu_2/e_{22})^{\frac{1}{2}}$. See figure 1. However, in the full four-dimensional space, B is,

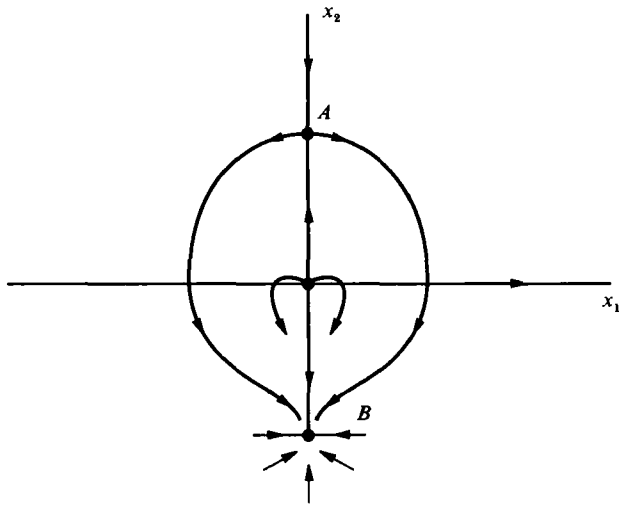

FIGURE 1. The first legs of the heteroclinic cycle.

like A, a saddle, but with unstable separatrices lying in the (y_1, x_2)-plane. This plane is the image under $a_j \to a_j \exp(\frac{1}{2}ij\pi)$, of the real subspace of figure 1 and, since (x_1, x_2) becomes $(y_1, -x_2)$ under this element of (2.4a), we conclude that there is a pair of orbits connecting B to A in the (y_1, x_2)-plane, thus completing the heteroclinic cycle.

In the integrable limit (2.2) these cycles correspond to the one-parameter family of solutions lying on the integral surface defined by $E = E_0 > 0$ and $L = 0$ (equation (2.3)). In the real subspace, which belongs to $L = 0$, they are the semi-ellipses $-\beta_{21} x_1^2 + \beta_{12} x_2^2 = E_0$, connecting $x_2 = \pm (E_0/(\beta_{12})^{\frac{1}{2}}$.

The five-mode boundary layer models of Aubry *et al.* (1988) and higher-dimensional systems, including non-zero streamwise wavenumbers, of Aubry & Sanghi (1989) possess similar heteroclinic cycles connecting fixed points which, restricted to the real subspace (now of dimension 5 or higher) are again saddles and sinks respectively (cf. Aubry *et al.* 1988, §10, figures 9 and 11 and Aubry & Sanghi (1989, figure 9).

If certain inequalities among the coefficients μ_j, β_{ij}, e_{ij} of (1.4) (and the analogues for (1.2)) are met, then the cycles are *attractive* in the sense that any solution starting near a cycle approaches it as $t \to +\infty$, spending increasing 'quasi-steady' periods near the saddle points, interspersed by rapid transitions in which the phases of the complex modes a_j shift by integer multiples of $\frac{1}{2}\pi$ or π. See §4, figure 2, for an example.

Aubry *et al.* (1988) pointed out that the intermittent events characteristic of heteroclinic cycles have much in common with the phenomenon of bursting in the boundary layer, in which quasi-steady streamwise vortices violently break up (locally) and subsequently reform, often with a lateral shift (Kline 1967, 1978). They also showed that the addition of weak quasi-random forcing to (1.2), corresponding to the fluctuating pressure field at the upper edge $x_2 = L_2$ of the wall region, introduces a typical timescale into the intermittency. Stone & Holmes (1989, 1990) subsequently provided a simple analysis of a randomly perturbed heteroclinic attractor and showed that the probability distribution of inter-event durations is skewed to the high end with an exponential tail, in agreement with some of the experimental evidence (Kim, Kline & Reynolds 1971; Bogard & Tiedermann 1986). Also see Holmes & Stone (1991) and Holmes (1991). Since heteroclinic cycles are a

robust feature of the models, 'stabilized' by the symmetries of the physical system, it is natural to suggest that they correspond to an important mechanism for the production of intermittency and bursting.

3. Energy production terms in coupled and uncoupled velocity fields

In order to see how the non-trivial fixed points and cycles of §2 arise, we must investigate the effects of the representation (1.1) on the projection process. We do this first for the coupled velocity components of the original model and then derive an uncoupled model.

3.1. *Representation by coupled velocity components*

We start from the Navier–Stokes equations for the evolution of perturbations $\boldsymbol{u}$ to the mean velocity field $\boldsymbol{U} = (U_1(x_2), 0, 0)$:

$$\partial u_i/\partial t = -U_{1,2}\,u_2\,\delta_{i1} - u_{1,1}\,U_1 - u_{i,j}\,u_j + \langle u_{i,j}\,u_j\rangle - (1/\rho)\,p_{,i} + \nu u_{i,jj}. \tag{3.1}$$

Here $\langle\ \rangle$ denotes the spatial average

$$\frac{1}{L_1 L_3}\int_0^{L_1}\int_0^{L_3}(\,)\,\mathrm{d}x_3\,\mathrm{d}x_1$$

and the mean velocity U_1 is assumed to have the form (1.3). Let

$$U_1^1 = \frac{u_\tau^2}{\nu}\left(x_2 - \frac{x_2^2}{H}\right) \tag{3.2}$$

denote the constant (pressure gradient) part of $U_1(x_2)$. Expanding the velocity field $\boldsymbol{u} = (u_1, u_2, u_3)$ in the form (1.1), substituting into (3.1) and taking the inner product,

$$(\boldsymbol{f}, \boldsymbol{g}) = \frac{1}{L_1 L_2 L_3}\int_0^{L_1}\int_0^{L_2}\int_0^{L_3}(f_i\,g_i^*)\,\mathrm{d}x_3\,\mathrm{d}x_2\,\mathrm{d}x_1, \tag{3.3}$$

with each basis vector $\exp(2\pi i l x_2/L_2)\,\phi_l(x_2)$, $l = -K, \ldots, K$, in turn, we obtain a set of $2K+1$ ordinary differential equations for the (scalar, complex) modal amplitude coefficients $a_{-K}, \ldots, a_K$. As noted in §1, reality of $\boldsymbol{u}$ and the fact that a_0 decays, implies that we need only consider the K equations for $a_1, \ldots, a_K$.

The driving term which destabilizes the trivial equilibrium $a_k = 0$ and leads to non-trivial equilibria and the related heteroclinic cycles derives from the term $-U_{1,2}\,u_2\,\delta_{i1}$ in (3.1). Projection of the linear part of this (cf. 3.2) yields

$$-\frac{1}{L_1 L_2 L_3}\int_0^{L_1}\int_0^{L_2}\int_0^{L_3}\left\{\frac{\partial U_1^1}{\partial x_2}(x_2)\sum_{k=-K}^{K} a_k(t)\exp(2\pi i(k-l)\,x_3/L_3)\begin{pmatrix}\phi_{2k}(x_2)\\0\\0\end{pmatrix}\cdot\begin{pmatrix}\phi_{1l}(x_2)\\\phi_{2l}(x_2)\\\phi_{3l}(x_2)\end{pmatrix}^*\right\}$$

$$\times\,\mathrm{d}x_3\,\mathrm{d}x_2\,\mathrm{d}x_1 = -\frac{a_l(t)}{L_2}\int_0^{L_2}\left(\frac{\partial U_1^1}{\partial x_2}(x_2)\,\phi_{2_l}(x_2)\,\phi_{1_l}^*(x_2)\right)\mathrm{d}x_2. \tag{3.4}$$

due to orthogonality of the Fourier components. Analogous expressions for the other linear terms, as well as quadratic and cubic ones, resulting from projection of (3.1) with $k_1 = 0$ and $\neq 0$, can be found in Aubry *et al.* (1988, Appendix A). The important point is that the other linear terms, derived from $\nu u_{i,jj}$, all have strictly negative coefficients whereas the expression (3.4) is positive, since ϕ_{2l} and ϕ_{1l} have opposite sign on $(0, L_2]$ for all l and U_1^1 is positive (Aubry *et al.* 1988, figure 4). These are the

terms $a_{ll} > 0$ of the diagonal entries $a_{ll} - \alpha(a'_{ll} + a''_{ll})$ of (1.2), which as α decreases, permit bifurcation of non-trivial equilibria. The 'production' terms are positive because the basis elements ϕ_l and the inner product (3.3) impose coupling among the velocity components. Energy input to the streamwise component u_1 via $-U_{1,2}u_2\delta_{i1}$ is forced to excite the cross-stream components u_2, u_3 by the restriction that admissible velocity fields have the form (1.1). We discuss this in terms of Reynolds stress in §3.3.

In (3.4) we only consider terms contributing to the matrix $\boldsymbol{A}_\alpha$ of (1.2), since we are primarily interested in the mechanism for destabilization of the trivial solution $\boldsymbol{a} = (\boldsymbol{u} =) 0$. However, we note that the full mean profile $\boldsymbol{U}$ of (1.3) is responsible for establishing non-trivial fixed points and heteroclinic cycles, via the cubic terms in $\boldsymbol{C}$ which derive from the Reynolds stress component of (1.3).

Before considering the effect of decoupling streamwise and cross-stream velocity components, we remark on the effect of including additional eigenfunctions in models with no streamwise variation. As the results of Herzog (1986) show (cf. Aubry *et al.* 1988, figure 2), representations of the form

$$\boldsymbol{u}(\boldsymbol{x}, t) = \boldsymbol{u}(x_2, x_3, t) = \sum_{k=-K}^{K} \sum_{n=1}^{N} a_k^{(n)}(t) \exp(2\pi i k x_3/L)\, \phi_k^{(n)}(x_2), \tag{3.5}$$

with no streamwise variations, would seriously fail to capture the typical energy content of the turbulent wall region. However, as $N, K \to \infty$ such an expansion must converge to the appropriate behaviour of 'two-dimensional' turbulence lacking streamwise variations. Velocity fields of the form $\boldsymbol{u}(x_2, x_3, t)$ do form an invariant subspace of the Navier–Stokes equations and the basis functions are a complete set. Hence, by Moffatt's (1990) arguments, if N and K are taken sufficiently large, the trivial solution should become globally attracting. In particular, the matrix $\boldsymbol{A}_\alpha$ of equation (1.2) should have entirely negative eigenvalues, even for small α.

While the eigenfunctions $\phi_l^{(n)}, \phi_k^{(m)}$ are mutually orthogonal with respect to the inner product (3.3), the expressions analogous to (3.4) involve $\partial U_1^1/\partial x_2$ as a weighting function and thus the 'production' term in the $a_l^{(n)}(t)$ equation resulting from the expansion (3.5) is in general

$$-\frac{1}{L_2} \sum_{m=1}^{N} a_k^{(m)} \int_0^{L_2} \left(\frac{\partial U_1}{\partial x_2}(x_2)\, \phi_{2_l}^{(m)}(x_2)\, \phi_{1_l}^{(n)*}(x_2) \right) \mathrm{d}x_2. \tag{3.6}$$

Herzog was only able to derive the first three families of eigenfunctions and the third is of questionable accuracy, but it appears that, for m or $n \geqslant 2$ the components $\phi_{2_l}^m \phi_{1_l}^n$ have the same sign over much of the range $0 < x_2 \leqslant L_2$, so that we expect contributions of the higher eigenfunctions to $\boldsymbol{A}_\alpha$ to be negative, and hence stabilizing. While not conclusive, this is consistent with the known physical properties of flows lacking streamwise variations, and with the fact that expansions of the form (3.5) are complete in the subspace of no streamwise variation, as $K, N \to \infty$.

3.2. *Representation by uncoupled velocity components*

We now wish to relax the restriction implicit in the representation (1.1) by permitting the streamwise and cross-stream components to evolve independently. This recovers the correct long-time behaviour of a flow lacking streamwise variations, even when only a single family of eigenfunctions is included. We will see that not only does a modest generalization of the model (1.2) reproduce this behaviour, but that it also reproduces significant features of the decay process and, incidentally, is of considerable independent interest.

We represent velocity fields in the form

$$\boldsymbol{u}(\boldsymbol{x},t) = \sum_{k=-K}^{K} \left[b_k(t) \exp(2\pi i k x_3/L_3) \begin{pmatrix} \phi_{1_k}(x_2) \\ 0 \\ 0 \end{pmatrix} + c_k(t) \exp(2\pi i k x_3/L_3) \begin{pmatrix} 0 \\ \phi_{2_k}(x_2) \\ \phi_{3_k}(x_2) \end{pmatrix} \right], \tag{3.7}$$

and, by projection onto the two sets of basis elements $(\phi_{1_k}, 0, 0)$ and $(0, \phi_{2_k}, \phi_{3_k})$ independently, produce $2(2K+1)$ ordinary differential equations for the evolution of the streamwise and cross-stream modal amplitudes b_k, c_k respectively. For convenience, we wish to select ϕ_{j_k} so that each basis element is divergence free and the pressure term of (3.1) can be removed (apart from the small boundary term) by integration by parts. Since the original empirical eigenfunctions (for $k_1 = 0$) are divergence free, satisfying

$$\frac{\mathrm{d}\phi_{2_k}}{\mathrm{d}x_2} + \frac{2\pi i k}{L_3} \phi_{3_k} = 0, \tag{3.8}$$

and, of course $(\partial/\partial x_1)(\exp(2\pi i k x_3/L_3)\,\phi_{i_k}(x_2)) \equiv 0$, this requirement is automatically met by these basis elements. Note, however, that they are no longer orthonormal, but merely satisfy

$$\left.\begin{aligned}
&\left(\exp(2\pi i l x_3/L_3) \begin{pmatrix} \phi_1 \\ 0 \\ 0 \end{pmatrix}, \exp(2\pi i k x_3/L_3) \begin{pmatrix} \phi_{1_k} \\ 0 \\ 0 \end{pmatrix}^* \right) \\
&\qquad = \frac{\delta_{lk}}{L_2} \int_0^{L_2} \{\phi_{1_l}(x_2)\, \phi_{1_k}^*(x_2)\} \mathrm{d}x_2 \overset{\text{def}}{=} B_l \delta_{lk}, \\
&\left(\exp(2\pi i l x_3/L_3) \begin{pmatrix} 0 \\ \phi_{2_l} \\ \phi_{3_l} \end{pmatrix}, \exp(2\pi i k x_3/k_3) \begin{pmatrix} 0 \\ \phi_{2_k} \\ \phi_{3_k} \end{pmatrix}^* \right) \\
&\qquad = \frac{\delta_{lk}}{L_2} \int_0^{L_2} \{\phi_{2_l}(x_2)\, \phi_{2_k}^*(x_2) + \phi_{3_l}(x_2)\, \phi_{3_k}^*(x_2)\} \mathrm{d}x_2 \overset{\text{def}}{=} C_l \delta_{lk} \\
&\left(\exp(2\pi i l x_3/L_3) \begin{pmatrix} \phi_{1_l} \\ 0 \\ 0 \end{pmatrix}, \exp(2\pi i l x_3/L_3) \begin{pmatrix} 0 \\ \phi_{2_k} \\ \phi_{3_k} \end{pmatrix}^* \right) = 0, \forall l, k,
\end{aligned}\right\} \tag{3.9}$$

although $B_l + C_l = 1$.

As Guckenheimer observes, if additional families of eigenfunctions $\phi_{i_k}^{\langle n \rangle}, n > 1$ are included in the representation, then orthogonality of the form (3.9) does not hold and there is no guarantee that the 'uncoupled' components are linearly independent. However, for the purposes of the present paper, this will not matter.

Using the representation (3.7), projection of $-U_{1,2} u_2 \delta_{i1}$ yields in the ordinary differential equation for $b_l(t)$:

$$-\frac{c_l(t)}{L_2} \int_0^{L_2} \left\{ \frac{\partial U_1(x_2)}{\partial x_2} \phi_{2_l}(x_2)\, \phi_{1_l}^*(x_2) \right\} \mathrm{d}x_2. \tag{3.10}$$

However, since

$$\int_0^{L_2} \left\{ \frac{\partial U_1(x_2)}{\partial x_2} c_k(t) \begin{pmatrix} \phi_{2_k}(x_2) \\ 0 \\ 0 \end{pmatrix} \cdot \begin{pmatrix} 0 \\ \phi_{2_l}(x_2) \\ \phi_{3_l}(x_2) \end{pmatrix}^* \right\} \mathrm{d}x_2 \equiv 0, \tag{3.11}$$

no such terms appear in the equations for the cross-stream components $c_l(t)$. The coefficients of the remaining linear terms are much as before, except that they now involve integrals of products of $\phi_{1_l}\phi_{1_l}^*$ and $(\phi_{2_l}\phi_{2_l}^* + \phi_{3_l}\phi_{3_l}^*)$ and their derivatives independently. The general expressions are given in Appendix A.

For a model involving two spanwise modes in b_l and c_l (four complex modes in all), the system takes the form

$$\left.\begin{aligned} \dot{b}_1 &= \lambda_1 b_1 + \rho_1 c_1 + \beta_{12} b_1^* c_2 + \beta_{11} b_2 c_1^* + c_1[e_{11}(b_1^* c_1 + b_1 c_1^* + e_{12}(b_2^* c_2 + b_2 c_2^*)], \\ \dot{b}_2 &= \lambda_2 b_2 + \rho_2 c_2 + \beta_{21} b_1 c_1 + c_2[e_{21}(b_1^* c_1 + b_1 c_1^*) + e_{22}(b_2^* c_2 + b_2 c_2^*)], \\ \dot{c}_1 &= \nu_1 c_1 + \gamma_{12} c_1^* c_2, \\ \dot{c}_2 &= \nu_2 c_2 + \gamma_{21} c_1^2, \end{aligned}\right\} \tag{3.12}$$

where, as in (2.1) the parameters u_j, ν_j, β_{ij}, γ_{ij}, e_{ij} are real. More generally, for K streamwise modes, the equations have the form

$$\left.\begin{aligned} \dot{\boldsymbol{b}} &= \boldsymbol{B}\boldsymbol{b} + \boldsymbol{D}\boldsymbol{c} + \boldsymbol{F}(\boldsymbol{c})\,\boldsymbol{b}, \\ \dot{\boldsymbol{c}} &= \boldsymbol{C}\boldsymbol{c} + \boldsymbol{E}(\boldsymbol{c}), \end{aligned}\right\} \tag{3.13}$$

where $\boldsymbol{B}, \boldsymbol{D}, \boldsymbol{F}$ and $\boldsymbol{C}$ are $K \times K$ diagonal matrices and $\boldsymbol{F}(\boldsymbol{c})$ and the vector $\boldsymbol{E}(\boldsymbol{c})$ depend on $\boldsymbol{c}$ quadratically. Note that the cross-stream modes, $\dot{\boldsymbol{c}}$, are decoupled and evolve independently and that the streamwise modes $\boldsymbol{b}$ form a linear system which is excited by the cross-stream modes. As expected, energy transfer from cross-stream to streamwise motions is possible, but not vice versa, in the absence of streamwise variations.

In writing (3.12) and (3.13) we have neglected the (real) perturbation component a_0 corresponding to the Fourier mode of zero spanwise wavenumber. This is, of course, simply a perturbation to the mean velocity. We have already allowed the disturbances to modify the mean velocity: this is the source of the cubic terms. The component a_0 is a dynamically empty term, which cannot be influenced by the rest of the system (although it can participate in the decay of b_j, c_j, discussed below). The component a_0 must be externally excited, and if excited, it simply decays, since the pressure gradient is only sufficient to support the unperturbed mean velocity. To excite a_0 would be, in effect, to consider a different problem – the behaviour of an uncoupled system in a decaying mean velocity. This problem may perhaps have its own interest, but not here and now – we are trying to construct an uncoupled system for comparison with the coupled system (2.1), and there a_0 is not included.

The structure of (3.12) with coupling from c_j to b_j but not vice versa, parallels that of the original Navier–Stokes equations (e.g. Moffatt 1990). In particular, the cross-stream modes c_j decay monotonically as we show in §4, and the streamwise modes b_j can (and do) initially grow in magnitude, extracting energy from the mean flow while the cross-stream modes are even minimally active. The basic mechanism was implicit in the considerations of Moffatt (1967) and later, in related work by Townsend (1970, 1976).

Since the basis elements of the representation (3.7) are derived from those of the coupled representation (1.1), various relationships obtain among the coefficients of

$\boldsymbol{B}, \boldsymbol{D}, \boldsymbol{F}, \boldsymbol{C}, \boldsymbol{E}$ of (3.13) and $\boldsymbol{A}, \boldsymbol{B}, \boldsymbol{C}$ of (1.2). Specifically, in the two mode cases (3.12) and (3.1), we find that the coefficients of the linear terms satisfy

$$B_j(\lambda_j+\rho_j)+(1-B_j)\,\nu_j = \mu_j \quad (j=1,2), \tag{3.14}$$

where $B_j\,(<1)$ is the quantity defined in (3.9). From the observations above (cf. (3.4) and (3.10)), and the expressions given in the Appendix, it is clear that

$$\lambda_j, \nu_j < 0 < \rho_j \tag{3.15}$$

and, if the viscosity ν is small, $\rho_j \gg |\lambda_j|, |\nu_j|$. In fact the ratios $|\rho_j/\lambda_j|$, $|\rho_j/\nu_j|$ are of the order of the Reynolds number for small dissipation to neglected modes. (If losses to the neglected modes are included, recall that eventually μ_j becomes negative, so that λ_j and ν_j and ρ_j are all of the same order for large α.) Relations analogous to (3.14) hold among the coefficients of quadratic and cubic terms (β_{ij}, e_{ij}) also. For reference, explicit expressions are given in the Appendix.

In the remainder of this paper we study the behaviour of the decoupled two-mode model (3.12) and compare it with that of the coupled model (2.1). Rather than seeking quantitatively accurate results, we wish to show that a low-order model of the type introduced by Aubry *et al.* (1988), lacking streamwise variations but allowing streamwise and cross-stream modes to evolve independently, correctly represents the qualitative features of decay of streamwise independent flows while still producing intermittency. In our numerical simulations, we have therefore not computed coefficients in (3.12) in detail but have merely selected representative values for both (2.1) and (3.12), satisfying the relations (3.14) and with appropriate relative magnitudes, as discussed above. The relevant facts are that, for single families of eigenfunctions, as Aubry *et al.* (1988) show, the cubic coefficients e_{ij} are all negative, and the quadratic coefficients of (2.1) satisfy:

$$\beta_{21} < 0 < \beta_{12}, \tag{3.16a}$$

and of (3.12):

$$\beta_{21} < 0 < \beta_{12}, \beta_{11}; \quad \gamma_{21} < 0 < \gamma_{12}. \tag{3.16b}$$

3.3. *A closure assumption in the coupled model*

We end this section by observing that the representation (1.1), involving the vector valued empirical eigenfunctions, effectively limits the ratio of Reynolds stress to energy. In particular, for K spanwise modes (using reality of $\boldsymbol{u}$), we have

$$\frac{\langle u_1 u_2\rangle}{\|u\|^2} = \frac{\sum_{k=1}^{K} a_k^2(t)\,\phi_{2_k}(x_2)\,\phi_{1_k}(x_2)}{\sum_{k=1}^{K}\sum_{j=1}^{3} a_k^2(t)\,|\phi_{jk}(x_2)|^2}, \tag{3.17}$$

which is bounded below and above by

$$\min_{k,l} \frac{\phi_{2_k}(x_2)\,\phi_{1_k}(x_2)}{\sum_{j=1}^{3}|\phi_{j_l}(x_2)|^2} \quad \text{and} \quad \max_{k,l} \frac{\phi_{2_k}(x_2)\,\phi_{1_k}(x_2)}{\sum_{j=1}^{3}|\phi_{j_l}(x_2)|^2}, \tag{3.18}$$

respectively. Since the product $\phi_{2_k}\phi_{1_k}$ of the empirical eigenvector components is non-zero on $(0, L_2]$ for all relevant k (Aubry *et al.* 1988, figure 4), this puts a strictly positive lower bound on $\langle u_1 u_2\rangle/\|u\|^2$ (at each $x_2 \in (0, L_2]$), regardless of the instantaneous values of the modal coefficients $a_k(t)$. Typical solutions a_k of the model equations give ratios considerably larger than this lower bound.

Recall that the empirical eigenfunctions are deduced from autocorrelation measurements in a turbulent boundary layer in which streamwise variations are

clearly present. Hence, in the 'coupled' model of Aubry *et al.* (1988), the eigenfunction expansion constitutes a closure approximation that embodies the effects of streamwise structure and unsteadiness in the values of $\langle u_1 u_2 \rangle / \|u\|^2$ represented by the relative magnitude of the eigenfunction components. In this sense the coupled model only *appears* to belong to the subspace of velocity fields lacking streamwise variation, since it incorporates a constraint which reflects the appropriate coupling between streamwise and cross-stream velocity components averaged over the streamwise direction x_1. This averaging is precisely equivalent to projection onto the subspace of streamwise wavenumber $k_1 = 0$. This latter point is addressed in greater depth in Holmes, Berkooz & Lumley (1991).

4. Analysis of the decoupled two-mode model

4.1. *Qualitative analysis*

We will not repeat the details of the analysis of the coupled two-mode model of (2.1), but merely quote relevant information from Armbruster *et al.* (1988). In that paper it is shown that rescaling of the coefficients e_{ij} allows us to set $\beta_{12} = -\beta_{21} = 1$. In that case, for

$$e_{ij} < 0,\ \mu_1, \mu_2 > 0,\ \mu_1 - \mu_2 e_{12}/e_{22} - (-\mu_2/e_{22})^{\frac{1}{2}} < 0 < \mu_1 - \mu_2 e_{12}/e_{22} + (-\mu_2/e_{22})^{\frac{1}{2}}$$

and $\mu_1 - \mu_2 e_{12}/e_{22} < 0$, the system possesses a family of attracting heteroclinic cycles connecting each diametrically opposite pair of saddle points on the circle of equilibria $|a_2| = (-\mu_2/e_{22})^{\frac{1}{2}}$. See figure 1 and figure 2.

As noted above, the structure of this system is closely related to that of the completely integrable (Hamiltonian) system

$$\dot{a}_1 = a_1^* a_2, \quad \dot{a}_2 = a_1^2, \tag{4.1}$$

obtained in the limit of small μ_j and a_j. This observation is also helpful in the decoupled model (3.12), for here the cross-stream modes (c_1, c_2) evolve autonomously, their governing equations being (after rescaling to set $\gamma_{12} = -\gamma_{21} = 1$):

$$\dot{c}_1 = \nu_1 c_1 + c_1^* c_2, \quad \dot{c}_2 = \nu_2 c_2 - c_1^2. \tag{4.2}$$

Using the functions E and L of (2.3a, b) (with $\beta_{12} = -\beta_{21} = 1$) which are constants of motion for $\nu_1 = \nu_2 = 0$, and recalling that these latter viscous dissipation terms are small (provided the loss to neglected modes, α, is not large), it is easy to describe the dynamical behaviour. Differentiating along solution curves, we obtain:

$$\left.\begin{aligned} E &= |c_1|^2 + |c_2|^2; \\ \frac{\mathrm{d}E}{\mathrm{d}t} &= \dot{c}_1 c_1^* + c_1 \dot{c}_1^* + \dot{c}_2 c_2^* + c_2 \dot{c}_2^* = 2(\nu_1 |c_1|^2 + \nu_2 |c_2|^2), \end{aligned}\right\} \tag{4.3}$$

and

$$\begin{aligned} L &= \mathrm{Im}\{c_1^2 c_2^* - c_1^{*2} c_2\}; \\ \frac{\mathrm{d}L}{\mathrm{d}t} &= \mathrm{Im}\{2c_1 \dot{c}_1 c_2^* + c_1^2 \dot{c}_2^* - 2c_1^* \dot{c}_1^* c_2 - c_1^{*2} \dot{c}_2\} \\ &= \mathrm{Im}\{(2\nu_1 + \nu_2)(c_1^2 c_2^* - c_1^{*2} c_2)\}, \end{aligned}$$

or

$$\frac{\mathrm{d}L}{\mathrm{d}t} = 2(2\nu_1 + \nu_2) L. \tag{4.4}$$

Letting $-\nu = \min\{-\nu_1, \nu_2\}$, (4.3) implies that

$$\mathrm{d}E/\mathrm{d}t \leqslant -2\nu E, \tag{4.5}$$

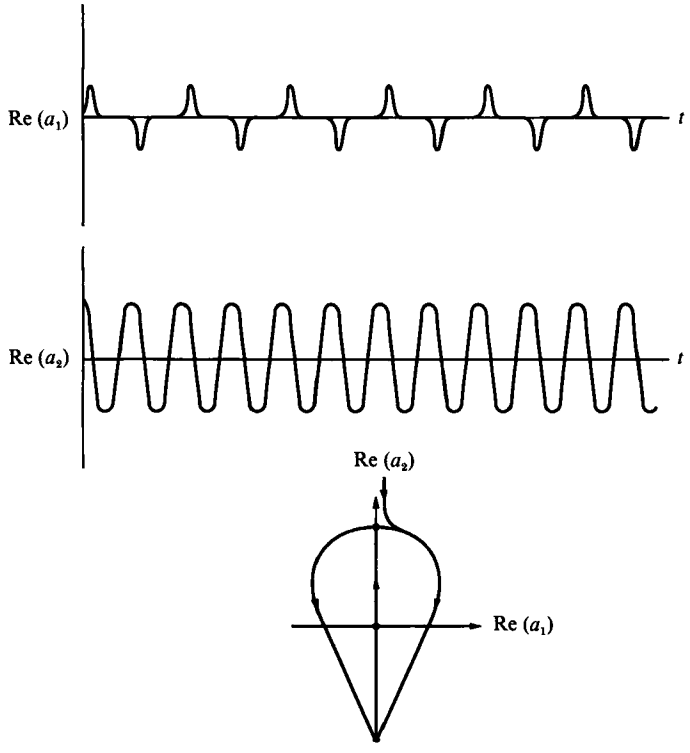

FIGURE 2. Evolution of modal components for the coupled model.

and thus, from (4.4) and (4.5), we conclude that both E and L are bounded above by exponential decay at rate determined by the viscous dissipation terms. Since E is a (positive definite, quadratic), Liapunov function for (4.2), it follows that all solutions approach the trivial fixed point $c_1 = c_2 = 0$ as $t \to \infty$. Consequently, as expected, the cross-stream velocity components decay.

Once c_1 and c_2 are arbitrarily small, the evolution of the streamwise components b_1, b_2 of (3.12) are also clear, since when $c_j = 0$ this equation reduces to

$$\dot{b}_1 = \lambda_1 b_1, \quad \dot{b}_2 = \lambda_2 b_2, \tag{4.6}$$

and, since the viscous terms λ_j are negative, we conclude that b_1 and b_2 also eventually decay to zero exponentially fast, in agreement with Moffatt (1990, equation (11). Regardless of the precise values of the coefficients in (3.12), the decoupled model therefore reproduces the correct asymptotic behaviour. We expect similar conclusions to hold for models including additional spanwise Fourier modes.

While the perturbation velocity field $\boldsymbol{u}$ of (3.7) eventually decays, its dynamical behaviour during this process is interesting. Since the dissipation parameters ν_j are small, the behaviour of the cross-stream components c_j is dominated by that of the integrable limit, which contains the families of heteroclinic orbits

$$E = |c_1|^2 + |c_2|^2 = E_0 > 0, \quad L = \mathrm{Im}\,(c_1 c_2^* - c_1^* c_2) = 0, \tag{4.7}$$

connecting each diametrically opposite pair of equilibrium on the circle $|c_2|^2 = E_0$, $c_1 = 0$. In the limit $\nu_j = 0$, almost all solutions near the heteroclinic cycles lie on periodic orbits of long period, corresponding to $L > 0$, small, most of the time being spent near the equilibria. A typical solution started near this circle will therefore slowly decay in 'energy' E, remaining close to $L = 0$, and so spending relatively long periods near the families of equilibria on $c_1 = 0$, punctuated by rapid transitions in

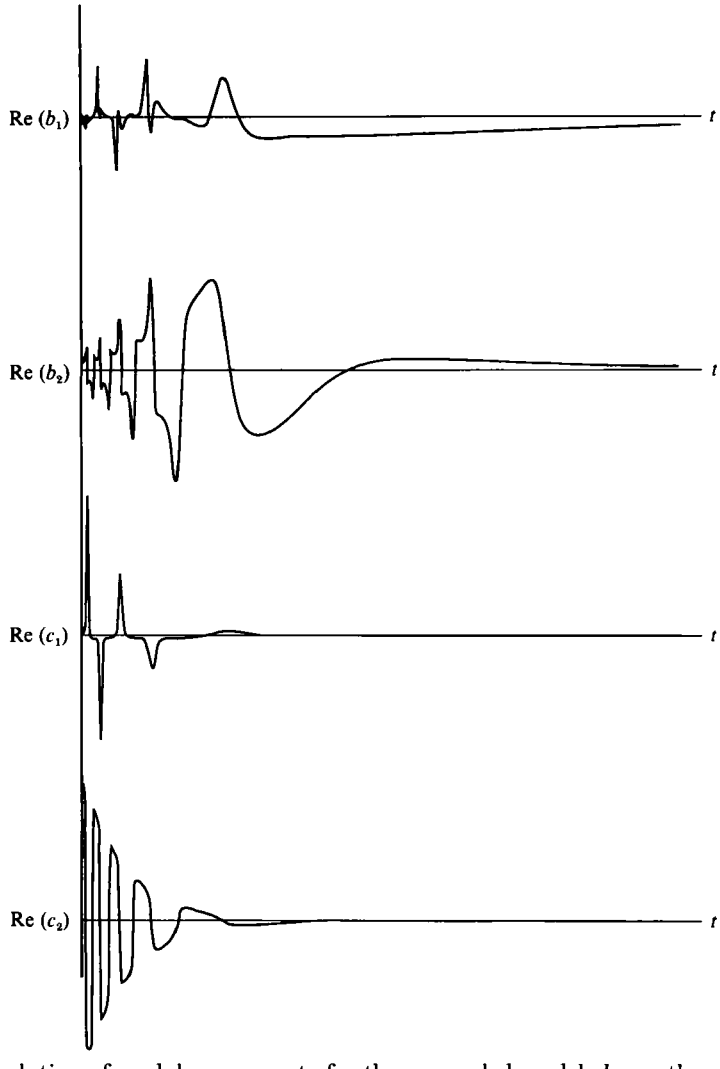

FIGURE 3. Evolution of modal components for the uncoupled model: b_j are the streamwise and c_j the cross-stream components respectively.

which c_1 grows and c_2 changes phase by π. The decay is not featureless, the heteroclinic cycles survive as a transient mechanism which transfers energy back and forth between the cross-stream Fourier modes.

The streamwise mode equation is rather harder to analyse, but, since the terms $\rho_j c_j$ which provide excitation have relatively large coefficients (recall that $|\rho_j/\lambda_j| \sim O(\mathrm{Re})$), we expect the weakly decaying energy in the cross-stream components to have a disproportionately large effect on the streamwise components. The numerical simulations, to which we now turn, show this to be the case, in agreement with other analyses, as remarked earlier.

4.2. *Numerical simulations*

As in the analysis of §4.1 shows, the general conclusions on solutions of the decoupled model (3.12) do not depend on the precise values of the coefficients, only on their signs and orders of magnitude. Rather than making detailed computations from

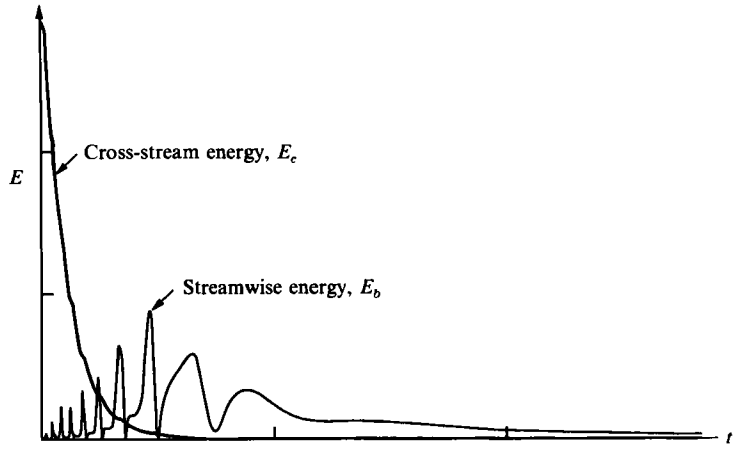

FIGURE 4. Evolution of energy for the uncoupled model.

Herzog's (1986) eigenvectors, we therefore merely fixed values in the appropriate ranges. For the results which follow we took

$$\lambda_1 = -1.2\times10^{-3}, \quad \lambda_2 = -2.4\times10^{-2}, \quad \rho_1 = 3.24\times10^{-2}, \quad \rho_2 = 6.48\times10^{-1},$$
$$\nu_1 = -6\times10^{-4}, \quad \nu_2 = -1.2\times10^{-2},$$
$$\beta_{12} = 0.75, \quad \beta_{11} = 0.75, \quad \beta_{21} = -0.5,$$
$$\gamma_{12} = 0.75, \quad \gamma_{21} = 0.75,$$
$$e_{11} = -12.0, \quad e_{12} = -3.0, \quad e_{21} = -6.0, \quad e_{22} = -6.0.$$

(Also see Armbruster *et al.* 1988). For comparison, a coupled model (3.1) was also integrated with the same choice of e_{ij} and corresponding values

$$\mu_1 = 0.01, \quad \mu_2 = 0.2, \quad \beta_{12} = 1, \quad \beta_{21} = -1.$$

Note that, taking $B_1 = B_2 = \frac{1}{3}$, the relations (3.14) hold. Integrations were performed using a fourth order Runge–Kutta method within the simulation environment 'kaos' by Kim & Guckenheimer (1990). A SUN sparcstation 1 was used.

Figure 2 shows a phase-plane projection and time series for the coupled system (2.1). Initial transients have been allowed to decay and the characteristic heteroclinic structure is clear (cf. Aubry *et al.* [1988, figure 9]). In contrast figure 3 shows solutions of the decoupled system, started with initial conditions

$$\mathrm{Re}\,(b_1) = \mathrm{Re}\,(c_1) = 0.01, \quad \mathrm{Im}\,(b_1) = \mathrm{Im}\,(c_1) = 0.01,$$
$$\mathrm{Re}\,(b_2) = \mathrm{Re}\,(c_2) = 1.0, \quad \mathrm{Im}\,(b_2) = \mathrm{Im}\,(c_2) = 0.01,$$

close to the cycle in the coupled model. As predicted, the exponential decay of $|c_2|$ is punctuated by rapid events in which $|c_1|$ grows and dies, each succeeding event being of lower magnitude. In contrast, the components b_j oscillate irregularly, exhibiting an overall increase in magnitude until the c_j are less than 1% of their original size. After this, the $|b_j|$ decay exponentially, as expected. The fact that the decay is slow is due to the relatively small (viscous) dissipation coefficients λ_j. The behaviour is perhaps best illustrated in figure 4, which shows the evolution of the cross-stream and streamwise energies $E_c = |c_1|^2 + |c_2|^2$ and $E_b = |b_1|^2 + |b_2|^2$ respectively. It is clear that the large coupling terms $\rho_j c_j$ allow E_b to increase even when the monotonically decaying E_c is rather small. This reflects the physical effect that even weak, non-zero, cross-stream velocities u_2, u_3 permit the extraction of energy from the mean flow U

by streamwise perturbations u_1, and the behaviour should be compared with that of the solution (1.4). As we have already noted, this behaviour has been remarked earlier, for example in the paper of Moffatt (1967).

5. Conclusions and physical implications

We briefly summarize the findings of this paper. Physical reasoning or direct analysis of the Navier–Stokes equations shows that perturbation velocity components lacking streamwise variations in the wall layer should decay, leaving only the mean velocity $\boldsymbol{U} = (U_1(x_2), 0, 0)$. The coupled empirical eigenfunction velocity components employed by Aubry *et al.* (1988) prevent this, since they permit continual energy extraction from the mean flow by holding the Reynolds stress/energy ratio $\langle u_1 u_2 \rangle / \|\boldsymbol{u}\|^2$ near its known mean value in the wall layer. In this way the effect of the streamwise variations on the production of turbulent kinetic energy are essentially averaged into the zero streamwise wavenumber eigenfunctions. The model of Aubry *et al.*, thus supplied continuously with energy, exhibits sustained intermittent (bursting) motions, corresponding to attracting heteroclinic cycles in phase space. These bursting motions mimic the bursting observed in the turbulent boundary layer, in particular the ejection and sweep phases.

When streamwise (u_1) and cross-stream (u_2, u_3) components are allowed to vary independently, as in the uncoupled model (3.12) of the present paper, we obtain the behaviour required of such a model without streamwise variation: the cross-stream components globally decay, while the streamwise component globally grows until the cross-stream components are essentially zero, whereupon it also decays. This behaviour, however, is strongly modified by 'ghosts' of the heteroclinic cycles, the cross-stream components exhibiting strong bursting on a timescale short relative to that of the decay. This bursting is the same phenomenon as that displayed by the model of Aubry *et al.* and can be identified as such in an otherwise identical coupled model.

For the parameters chosen (whose relative magnitudes are physically reasonable), the decay of the cross-stream energy is rapid relative to the eventual decay of the streamwise energy. This suggests that the presence of cross-stream components and their bursting would occupy a relatively small fraction of the time and space in a real flow, while the decaying streamwise components (which take the form of low-speed streaks) would be present in a much larger fraction of time and space. The first observers of the bursting phenomenon referred primarily to the 'low-speed streak' (e.g. Hama & Corrsin 1957; Kline *et al.* 1967). It was only later (Bakewell & Lumley 1967; Willmarth 1975; Blackwelder & Eckelmann 1979) that streamwise counter-rotating eddy pairs were associated with the low-speed streaks. There is still controversy over which produces which, and many observers consider the low-speed streaks to be primary, although we do not (see the discussion for the Coherent Structure session in Lumley (1990), particular Kline's remarks).

This study demonstrates that the intermittent dynamics associated with heteroclinic cycles survives even in a class of models whose uncoupled velocity components eventually decay. In fact, the cycles are a direct consequence of natural physical symmetries and of the quadratic interaction terms in the Navier–Stokes equations, as the integrable limiting cases (2.2) and (4.1) demonstrate. The main features causing intermittency and bursting in the original model of Aubry *et al.* are therefore independent of the closure assumption inherent in the use of empirical eigenfunctions. This work also shows that low-dimensional projections of the

Navier–Stokes equations, restricted to subspaces lacking streamwise variations, can adequately capture the dynamics of decaying turbulence. However, we conclude by stressing that, in order to reproduce the sustained dynamical interactions characteristic to the wall layer, which depend upon streamwise variations, in a low-dimensional model, one must incorporate streamwise effects in a suitably averaged fashion. As we show in §3.3, the empirical eigenfunctions of the proper orthogonal decomposition provide the appropriate averaging procedure.

It is important to note that, while the empirical eigenfunctions are stationary velocity fields obtained by averaging, their variable coefficients, evolving via the truncated Navier–Stokes equations, produce instantaneous dynamical behaviours characteristic of the full flow (Aubry *et al.* 1988; Aubry & Sanghi 1989, 1990). A qualitative measure of how faithful such models are would require one to average the amplitude coefficients of the model equations and compare their ratios with those of the empirical eigenvalues, which are characteristic of the full flow. Studies of this, and of projections of direct numerical simulations onto empirical subspaces in comparison with solutions of low-dimensional projected equations, are currently in progress.

This paper was motivated by the comments of H. K. Moffatt at the conference *Whither Turbulence?*, held in Ithaca in March 1989 (see Moffatt 1990; Lumley 1990). Parts of the material appeared as an author's closure in the proceedings of that conference (Holmes 1990). The work was carried out under AFOSR contract 89-0226A (Wall Layers).

Appendix A. Decoupled equations and constraints on coefficients

For one eigenfunction and an arbitrary number of cross-stream Fourier modes and no streamwise modes the Navier–Stokes equations (with the mean velocity profile expressed in terms of the Reynolds stress) have the following terms after projection. (*Note:* different notation to that used in text.)

A.1. *Coupled case*

We perform a Galerkin projection on the subspace spanned by

$$\frac{1}{(L_1 L_3)^{\frac{1}{2}}}\exp(2\pi i x_3 k_3/L_3)\,(\phi_{1_{k_3}}(x_2), \phi_{2_{k_3}}(x_2), \phi_{3_{k_3}}(x_2)),$$

using $(k = k_3)$

$$\int_0^{X_2} \phi_{i_k}(x_2)\,\phi_{i_k}^*(x_2)\,\mathrm{d}x_2 = \delta_{k,k}.$$

The resulting equations have the forms:

$$\dot{a}_k = -4\pi^2\left(\frac{k}{L_3}\right)^2 a_k + a_k\left[\int_0^{X_2}\frac{\mathrm{d}^2\phi_{i_k}}{\mathrm{d}x_2^2}\phi_{i_k}^*\,\mathrm{d}x_2 - \int_0^{X_2}\phi_{2_k}\phi_{1_k}^*\left(1-\frac{2x_2}{H}\right)\mathrm{d}x_2\right]$$

$$-\sum_{k'} a_{k'}a_{k-k'}(1-\delta_{k',0})\int_0^{X_2}\left[2\pi i\frac{k'}{L_3}\phi_{i_{k'}}\phi_{3_{k-k'}} + \frac{\mathrm{d}\phi_{i_{k'}}}{\mathrm{d}x_2}\phi_{2_{k-k'}}\right]\phi_{i_k}^*\,\mathrm{d}x_2$$

$$-\sum_{k'} a_k a_{-k'} a_{k'}\int_0^{X_2}\phi_{1_{k'}}\phi_{2_{k'}}\phi_{2_k}\phi_{1_k}^*\,\mathrm{d}x_2 - \hat{p}_k(X_2,t)\,\phi_{2_k}^*(X_2) = B_k a_k + \sum_{k'} C_{k,k'}a_{k'}a_{k-k'}$$

$$+\sum_{k'=-\infty}^{\infty} D_{k,k'}a_k a_k a_{-k'} + f_k(t).$$

Here $f_k(t)$ is a forcing term due to the matching to the outer layer. The symmetries of the system have not been used to express it in a simpler form, as done in Aubry *et al.* (1988).

A.2. *Uncoupled case*

We perform a Galerkin projection on the subspaces spanned by

$$\frac{1}{(L_1 L_3)^{\frac{1}{2}}}\exp(2\pi i x_3 k_3/L_3)\,(\phi_{i_{k_3}}(x_2),0,0)$$

and

$$\frac{1}{(L_1 L_3)^{\frac{1}{2}}}\exp(2\pi i x_3 k_3/L_3)(0,\phi_{2_{k_3}}(x_2),\phi_{3_{k_3}}(x_2)),$$

and get ($k \equiv k_3$)

$$\begin{aligned}
\dot{b}_k = {} & \frac{1}{\int_0^{X_2}\phi_{1_k}\phi_{1_k}^*\,\mathrm{d}x_2}\Bigg[-4\pi^2\left(\frac{k}{L_3}\right)^2 b_k\int_0^{X_2}\phi_{1_k}\phi_{1_k}^*\,\mathrm{d}x_2 + b_k\int_0^{X_2}\frac{\mathrm{d}^2\phi_{1_k}}{\mathrm{d}x_2^2}\phi_{1_k}^*\,\mathrm{d}x_2 \\
& - c_k\int_0^{X_2}\phi_{2_k}\left(1-\frac{2x_2}{H}\right)\phi_{1_k}^*\,\mathrm{d}x_2 \\
& - \sum_{k'}(1-\delta_{k',0})\,b_{k'}c_{k-k'}\int_0^{X_2}\left(2\pi i\frac{k'}{L_3}\phi_{1_{k'}}\phi_{3_{k-k'}}\phi_{1_k}^* + \frac{\mathrm{d}\phi_{1_{k'}}}{\mathrm{d}x_2}\phi_{2_{k-k'}}\phi_{1_k}^*\right)\mathrm{d}x_2 \\
& - \sum_{k'} b_{k'}c_{-k'}c_k\int_0^{X_2}\phi_{1_{k'}}\phi_{2_{-k'}}\phi_{2_k}\phi_{1_k}^*\,\mathrm{d}x_2\Bigg] \\
= {} & \frac{1}{\alpha_k}[E_k b_k + F_k c_k + \sum_{k'} b_{k'}c_{k-k'}G_{k,k'} + \sum_{k'} b_{k'}c_{-k'}c_k H_{k,k'}] \\
= {} & \frac{1}{\alpha_k}\Bigg[E_k b_k + F_k c_k + \sum_{k'=-\infty}^{\infty} b_{k'}(c_{k-k'}G_{k,k'} + c_{-k'}c_k H_{k,k'})\Bigg].
\end{aligned}$$

$$\begin{aligned}
\dot{c}_k = {} & \frac{1}{\int_0^{X_2}(\phi_{2_k}\phi_{2_k}^* + \phi_{3_k}\phi_{3_k}^*)\,\mathrm{d}x_2}\Bigg[-4\pi^2\left(\frac{k}{L_3}\right)^2 c_k\int_0^{X_2}(\phi_{2_k}\phi_{2_k}^* + \phi_{3_k}\phi_{3_k}^*)\,\mathrm{d}x_2 \\
& + c_k\int_0^{X_2}\left(\frac{\mathrm{d}^2\phi_{2_k}}{\mathrm{d}x_2^2}\phi_{2_k}^* + \frac{\mathrm{d}^2\phi_{3_k}}{\mathrm{d}x_2^2}\phi_{3_k}^*\right)\mathrm{d}x_2 \\
& + \sum_{k'} c_{k-k'}c_{k'}\int_0^{X_2}\Bigg(\phi_{2_{k-k'}}\left(\frac{\mathrm{d}}{\mathrm{d}x_2}\phi_{3_{k'}}\phi_{3_k}^* + \frac{\mathrm{d}}{\mathrm{d}x_2}\phi_{2_{k'}}\phi_{2_k}^*\right) \\
& + 2\pi i k'\phi_{3_{k-k'}}(\phi_{2_{k'}}\phi_{2_k}^* + \phi_{3_{k'}}\phi_{3_k}^*)\Bigg)\mathrm{d}x_2 - \hat{p}_k(X_2)\,\phi_{2_k}(X_2)\Bigg] \\
= {} & \frac{1}{\beta_k}\Bigg[I_k c_k + \sum_{k'=-\infty}^{\infty} J_{k,k'}c_{k-k'}c_{k'} + g_k(t)\Bigg].
\end{aligned}$$

The following constraints apply:

$$\alpha_k + \beta_k = 1, \quad \alpha_k > 0, \quad \beta_k > 0.$$

$$E_k + F_k + I_k = B_k, \quad I_k < 0 \text{ and } E_k < 0$$

are damping terms, $F_k > 0$ is a driving term. In the equations studied $B_k > 0$. Also:

$$G_{k,k'} + J_{k,k'} = C_{k,k'}, \quad H_{k,k} = D_{k,k}, \quad g_k(t) = f_k(t).$$

The outer layer perturbation pressure term appears only in the cross-stream equation.

Recall that the equations studied in Aubry *et al.* (1988) had 'Heisenberg damping terms'. Those included both linear and quadratic terms. We assume they split in a similar manner in the present case. To get the equations studied one should observe that the realizability implies that $c_{-k}\phi_{i_{-k}} = c_k^* \phi_{i_k}^*$ (see Aubry *et al.* 1988) thus it is enough to study b_k, c_k for $k > 0$. Also note that the new systems have the $O(2)$ symmetry of the original system, but in a new representation: i.e. for any θ, $(b_j, c_j) \to (e^{ij\theta} b_j, e^{ij\theta} c_j)$ is a symmetry. The coefficients of the equations are real for the same reasons described in Aubry *et al.*

REFERENCES

ARMBRUSTER, D., GUCKENHEIMER, J. & HOLMES, P. 1988 Heteroclinc cycles and modulated travelling waves in systems with $O(2)$ symmetry. *Physica* **29**D, 257–282.

ARMBRUSTER, D., GUCKENHEIMER, J. & HOLMES, P. 1989 Kuramoto–Sivashinsky dynamics on the center unstable manifold. *SIAM J. Appl. Maths* **49**, 676–691.

AUBRY, N. & SANGHI, S. 1989 Streamwise and spanwise dynamics of the turbulent wall layer. In *Forum on Chaotic Flow* (ed. X. Ghia), Proc. ASME, New York.

AUBRY, N. & SANGHI, S. 1990 Bifurcation and bursting of streaks in the turbulent wall layers. In Turbulence 89: *Organized Structures and Turbulence in Fluid Mechanics* (ed. M. Lesieur & O. Métais). Kluwer.

AUBRY, N., HOLMES, P. & LUMLEY, J. L. 1990 The effect of modeled drag reduction on the wall region. In *Theoretical and Computational Fluid Dynamics*, vol. 1, pp. 229–248. Springer.

AUBRY, N., HOLMES, P. & LUMLEY, J. L. & STONE, E. 1988 The dynamics of coherent structures in the wall region of a turbulent boundary layer. *J. Fluid Mech.* **192**, 115–173.

BAKEWELL, P. & LUMLEY, J. L. 1967 Viscous sublayer and adjacent wall region in turbulent pipe flows. *Phys. Fluids* **10**, 1880–1889.

BLACKWELDER, R. F. & ECKELMANN, H. 1979 Streamwise vortices associated with the bursting phenomenon. *J. Fluid Mech.* **94**, 577–594.

BOGARD, D. G. & TIEDERMAN, W. G. 1986 Burst detection with single point velocity measurements. *J. Fluid Mech.* **162**, 389–413.

BUSSE, F. M. 1981 Transition to turbulence in Rayleigh–Bénard convection. In *Hydrodynamic Instabilities and the Transition to Turbulence* (ed. H. L. Swinney & J. P. Gollub), pp. 97–137. Springer.

BUSSE, F. M. & HEIKES, K. E. 1980 Convection in a rotating layer: a simple case of turbulence. *Science* **208**, 173–175.

CORINO, E. R. & BRODKEY, R. S. 1969 A visual investigation of the wall region in turbulent flows. *J. Fluid Mech.* **37**, 1–30.

CORRSIN, S. 1957 Some current problems in shear flows. In *Proc. Naval Hydr. Symp. 24–28 Sept. 1956*, (ed. F. S. Sheman).

GUCKENHEIMER, J. & HOLMES, P. 1983 *Nonlinear oscillations, dynamical systems and bifurcations of vector fields*. Springer. (Corrected 3rd printing, 1990.)

GUCKENHEIMER, J. & HOLMES, P. 1988 Structurally stable heteroclinic cycles. *Math. Proc. Camb. Phil. Soc.* **103**, 189–192.

GUCKENHEIMER, J. & KIM, S. 1990 Kaos. *MSI Tech. Rep.* 90–15. Cornell University, Ithaca, NY.

HERZOG, S. 1986 The large scale structure in the near-wall region of turbulent pipe flow. PhD thesis, Cornell University, Ithaca, N.Y.

HOLMES, P. 1990 Can dynamical systems approach turbulence? In *Proc. Whither Turbulence?*

Turbulence at the Crossroads (ed. J. L. Lumley). Lecture Notes in Applied Physics, vol. 357, pp. 197–249, 306–309. Springer.

HOLMES, P. 1991 Symmetries, heteroclinic cycles and intermittency in fluid flow. In *Proc. I.M.A. Workshop on Dynamical Theories of Turbulence in Fluid Flows* (to appear). Springer.

HOLMES, P., BERKOOZ, G. & LUMLEY, J. L. 1991 Turbulence, dynamical systems and the unreasonable effectiveness of empirical eigenfunctions. In *Proceedings of the International Congress of Mathematicians ICM-90*. Springer (to appear).

HOLMES, P. & STONE, E. 1991 Heteroclinic cycles, exponential tails and intermittency in turbulence production. In *Proc. Symp. in Honor of J. L. Lumley* (to appear). Springer.

HYMAN, J. M. & NICOLAENKO, B. 1985 The Kuramoto–Sivashinsky equation: a bridge between PDE's and dynamical systems. *Los Alamos National Lab Report LA-UR-85-1556*.

HYMAN, J. M., NICOLAENKO, B. & ZALESKI, S. 1986 Order and complexity in the Kuramoto–Sivashinsky model of weakly turbulent interfaces. *Los Alamos National Lab Report LA-UR-86-1947*.

JONES, C. & PROCTOR, M. R. 1987 Strong spatial references and travelling waves in Bénard convection. *Phys. Lett.* A **121**, 224–227.

KIM, H. T., KLINE, S. J. & REYNOLDS, W. C. 1971 The production of turbulence near a smooth wall in a turbulent boundary layer. *J. Fluid Mech.* **50**, 133–160.

KIRBY, M., BORIS, J. P. & SIROVICH, L. 1990 A proper orthogonal decomposition of a simulated supersonic shear layer. *Intl J. for Numer. Math. Fluids* **10**, 411–428.

KLINE, S. J. 1967 Observed structure features in turbulent and transitional boundary layers. *Fluid Mechanics of Internal Flow* (ed. G. Sovran), pp. 27–68. Elsevier.

KLINE, S. J. 1978 In *Coherent Structure of Turbulent Boundary Layers*, Proc. AFOSR/Lehigh Workshop (ed. C. R. Smith and D. E. Abbott), pp. 1–26. The role of visualization in the study of the turbulent boundary layer.

KLINE, S. J., REYNOLDS, W. C., SCHRAUB, F. A. & RUNDSTADLER, P. W. 1967 The structure of turbulent boundary layers. *J. Fluid Mech.* **30**, 741–773.

LADYZHENSKAYA, O. A. 1969 *The Mathematical Theory of Viscous Incompressible Flows*. Gordon and Breach.

LUMLEY, J. L. 1967 The structure of inhomogeneous turbulent flows. In *Atmospheric Turbulence and Radio Wave Propagation* (ed. A. M. Yaglom & V. I. Tatarski), pp. 166–178. Moscow: Nauka.

LUMLEY, J. L. 1970 *Stochastic Tools in Turbulence*. Academic.

LUMLEY, J. L. (ED.) 1990 *Whither Turbulence? Turbulence at the Crossroads*. Springer Lecture Notes in Physics (to appear).

MOFFATT, H. K. 1967 The interaction of turbulence with strong wind shear. In *Atmospheric Turbulence and Radio Wave Propagations* (ed. A. M. Yaglom & V. I. Tatarsky), pp. 139–156. Moscow: Nauka.

MOFFATT, H. K. 1990 Fixed points of turbulent dynamical systems and suppression of nonlinearity. In *Whither Turbulence? Turbulence at the Crossroads* (ed. J. L. Lumley), pp. 250–257. Lecture Notes in Applied Physics, vol. 357. Springer.

MOIN, P. & MOSER, R. D. 1989 Characteristic-eddy decomposition of turbulence in a channel. *J. Fluid Mech.* **200**, 471–509.

NEWELL, A. C., RAND, D. A. & RUSSELL, D. 1988 Turbulent transport and the random occurrence of coherent events. *Physica* **33D**, 281–303.

NICOLAENKO, B. & SHE, Z. S. 1990*a* Temporal intermittency and turbulence production in the Kolomogorov flow. In *Topological Dynamics of Turbulence*. Cambridge University Press.

NICOLAENKO, B. & SHE, Z. S. 1990*b* Symmetry-breaking homoclinic chaos in Kolomogorov flows. Preprint, Arizona State University.

NICOLAENKO, B., SCHEURER, B. & TÉMAN, R. 1985 Some global dynamical properties of the Kuramoto–Sivashinsky equations: nonlinear stability and attractors. *Physics* **1bD**, 155–183.

NICOLAENKO, B., SCHEURER, B. & TÉMAN, R. 1986 Attractors for the Kuramoto–Sivashinsky equations. *Los Alamos National Lab. Report LA-UR-85-1630*.

PROCTOR, M. R. & JONES, C. 1988 The interaction of two spatially resonant patterns in thermal convection. *J. Fluid Mech.* **188**, 301–335. Part 1. Exact 1:2 resonance.

SIROVICH, L. 1989 Chaotic dynamics of coherent structures. *Physica* **37D**, 126–145.

STONE, E. 1989 Studies of low dimensional models for the wall region of a turbulent boundary layer. PhD thesis, Cornell University, Ithaca, NY.

STONE, E. & HOLMES, P. 1989 Noise induced intermittency in a model of a turbulent boundary. *Physica* **37D**, 20–32.

STONE, E. & HOLMES, P. 1990 Random perturbation of heteroclinic attractors. *SIAM J. Appl. Maths.* **50**, 726–743.

TÉMAN, R. 1988 *Infinite-Dimensional Dynamical Systems in Mechanics and Physics.* Springer.

TOWNSEND, A. A. 1970 Entrainment and structure of turbulent flow. *J. Fluid Mech.* **41**, 13–46.

TOWNSEND, A. A. 1976 *Structure of Turbulent Shear Flows* (2nd edn). Cambridge University Press.

WILLMARTH, W. W. 1975 Structure of turbulence in boundary layers. *Adv. Appl. Mech.* **15**, 159–254.